Translational Oncology
www.transonc.com

Volume 4 Number 1 February 2011 pp. 20–28 20

CXCR2-Dependent Endothelial Progenitor Cell Mobilization in Pancreatic Cancer Growth[1]

Aihua Li*, Xiao J. Cheng*, Aune Moro*, Rakesh K. Singh†, Oscar Joe Hines* and Guido Eibl*

*Department of Surgery, David Geffen School of Medicine, University of California at Los Angeles, Los Angeles, CA, USA; †Department of Pathology and Microbiology, University of Nebraska Medical Center, Omaha, NE, USA

Abstract

Neovascularization is essential for tumor growth. We have previously reported that the chemokine receptor CXCR2 is an important regulator in tumor angiogenesis. Here we report that the mobilization of bone marrow (BM)–derived endothelial progenitor cells (EPCs) is impaired in CXCR2 knockout mice harboring pancreatic cancers. The circulating levels of EPCs (positive for CD34, CD117, CD133, or CD146) are decreased in the bone marrow and/or blood of tumor-bearing CXCR2 knockout mice. CXCR2 gene knockout reduced BM-derived EPC proliferation, differentiation, and vasculogenesis *in vitro*. EPCs double positive for CD34 and CD133 increased tumor angiogenesis and pancreatic cancer growth *in vivo*. In addition, $CD133^+$ and $CD146^+$ EPCs in human pancreatic cancer are increased compared with normal pancreas tissue. These findings indicate a role of BM-derived EPC in pancreatic cancer growth and provide a cellular mechanism for CXCR2 mediated tumor neovascularization.

Translational Oncology (2011) 4, 20–28

Introduction

Endothelial progenitor cells (EPCs) originate mainly from the bone marrow–derived cells with the ability to differentiate into mature endothelial cells and contribute to blood vessel formation. The bone marrow consists of many cell types [1], of which EPCs, pericyte progenitor cells [2], myeloid progenitor cells [3], dendritic progenitor cells [4], and tumor-associated macrophages [5,6] have been involved in tumor vasculogenesis and promotion of tumor growth. Whereas some types of BM-derived cells contribute to tumor neovascularization indirectly by providing structural support, EPCs play a central role in tumor vasculogenesis. Initially, EPCs were identified in vasculogenesis during embryogenesis but are now recognized to be important to vessel formation in adulthood as well. Since EPCs were first isolated as $CD34^+$ cells from human peripheral blood in 1997 [7], increasing evidence demonstrated the role of EPC-mediated postnatal vasculogenesis in various pathologic conditions including cardiovascular disease, wound healing, and tumor neovascularization. In general, EPCs express three surface markers CD34, CD133, and vascular endothelial growth factor receptor 2 (VEGFR2). These cells characterize the early functional angioblast in the bone marrow. In addition, CD117, CD146, VE-cadherin, and Tie-2 are also expressed on EPCs [8–10]. Recent evidences demonstrated that BM-derived EPCs play an important role in tumor neovascularization, tumor growth, and metastasis [10,11]. Tumor neovascularization is a complex process. It is composed of angiogenesis by sprouting of local endothelial cells and vasculogenesis by BM-derived EPCs. The functional role of EPCs in tumor neovascularization has been demonstrated in several cancer models including lung cancer, lymphoma, breast cancer, melanoma, insulinoma, and brain tumor [12–17]. By using the EPC defective Id1+/–Id3–/– mice, Lyden et al. [12] demonstrated that EPCs are necessary for tumor vasculogenesis and growth in mouse lung cancer and lymphoma. The BM-derived EPCs incorporated into early stage tumor vessel and contributed to lung cancer, breast cancer, and melanoma growth [13,14]. Moreover, Kaplan et al. and Gao et al. [15] established an important role of EPCs in lung metastasis of breast cancer. In a spontaneous insulinoma model, Spring et al. [16] showed that EPCs incorporated into the tumor vessel and contributed to the late stage of tumor growth. Du et al. [17] observed recruitment of hypoxia-inducible 1–induced BM-derived EPCs into tumor site and initiation of the angiogenic switch by EPCs in an orthotopic brain tumor model.

Address all correspondence to: Aihua Li, MD, PhD, Department of Surgery, David Geffen School of Medicine, University of California at Los Angeles, 675 Charles Young Dr S, MRL 2535, Los Angeles, CA 90095. E-mail: 2006.aihua@gmail.com

[1]This work was supported by grants R21 CA124609 (O.J. Hines) and R01 CA122042 (G. Eibl) from the National Institutes of Health.
Received 24 June 2010; Revised 9 October 2010; Accepted 13 October 2010

1944-7124/11
DOI 10.1593/tlo.10184

Chemokines with a C-X-C cystein motif have angiogenic function and are involved in tumor growth and metastasis [18,19]. We and others have shown that the CXC chemokine ligands CXCL5 (ENA-78) and CXCL8 (IL-8) interact with its common receptor CXCR2 stimulating angiogenesis, involved in tumor growth and metastasis in broad types of cancer including colon cancer, lung cancer, and pancreatic cancer [18–24]. The tumor-promoting effect of the CXCL5/CXCL8/CXCR2 axis has been shown to signal through activation of NF-κB and phosphorylation of mitogen-activated kinases and phosphoinositide-3 kinase [21,22]. However, the cellular and molecular mechanisms of CXCL5/CXCL8/CXCR2–mediated angiogenesis and tumor growth are not fully understood.

Although the contribution of EPC to tumor neovascularization has been demonstrated in several types of cancer, the role of BM-derived EPC in pancreatic adenocarcinoma and the regulation of EPC mobilization by CXCR2 in tumor neovascularization have not been reported. The aim of this study was to determine the role of CXCR2 on regulation of EPC mobilization and function. Our data showed that BM-derived EPCs stimulated vasculogenesis and pancreatic cancer growth. EPCs are mobilized by pancreatic cancer cells. CXCR2 gene knockout impaired EPC mobilization and reduced EPC proliferation, differentiation, and neovascularization.

Materials and Methods

Cell Lines and Reagents

Mouse pancreatic cancer cells harboring a Kras mutation (G12D) [25] were a kind gift from Dr Ashok Saluja (University of Minnesota). The cell line was maintained in culture as an adherent monolayer in RPMI supplemented with 10% fetal bovine serum. CD34, CD117, CD133, CD146, and isotype IgG control antibodies for flow cytometry were purchased from eBioscience (San Diego, CA). Antibodies to human CD133 or CD146 for immunohistochemistry were obtained from Abcam (Cambridge, MA). Anti–mouse CD31 antibody was from Angio-Proteomie (Boston, MA).

Patient Specimens

Nine cases of paired pancreatic tumor/normal pancreas and eight cases of unpaired tumors or normal pancreas (formalin-fixed, paraffin-embedded) samples from 1989 to 2005 were obtained through the University of California at Los Angeles (UCLA), Departments of Surgery and Pathology. This study was approved by the Institutional Review Board at the UCLA, School of Medicine.

Mice

CXCR2 knockout mice were generated by crossing CXCR2 heterozygous mice (Jackson laboratory) on C57 mouse background. Genotyping analysis was done using mouse tail DNA. Polymerase chain reaction (PCR) primers were as follows: CXCR2 wild type, 5′-GGT CGT ACT GCG TAT CCT GCC TCA G and 3′-TAG CCA TGA TCT TGA GAA GTC CAT G; and CXCR2 mutant, 5′-CTT GGG TGG AGA GGC TAT TC and 3′-AGG TGA GAT GAC AGG AGA TC. Tail DNA was extracted by a genotyping preparation kit, and PCR was carried out using the 2× Taq PCR Premix (Bioland Scientific, San Diego, CA). PCR products were separated on a 2% agarose gel. All animal housing, care, and experiments were performed in accordance with institutional guideline and approved by the UCLA Institutional Animal Care and Use Committee.

In Vitro *Cell Proliferation Assay*

Bone marrow (BM) was flashed out from tibias and femurs of mice, washed with Dulbecco modified Eagle medium containing 5% FBS. Red blood cells were lysed with RBC lysis buffer (Sigma, St Louis, MO). After washing with PBS, mononuclear cells (10^5) were collected and cultured in suspension with endothelial growth medium (EGM; Lanzo, Allendale, NJ) for 6 days. Cell growth was measured by cell counting with Trypan blue.

In Vitro *Cell Differentiation and Angiogenesis Assay*

BM mononuclear cells (2×10^4) were seeded into 24-well culture plate coated with fibronectin or Matrigel and cultured with EGM with or without mouse pancreatic cancer–conditioned medium (PCCM). After 4 to 6 days, the plate was examined for differentiated cells or capillary tube formation and photographed. Total tube length was determined by image analysis software (Image J; National Institutes of Health, Bethesda, MD). The qualitative difference in tube formation was examined. Each assay was done in duplicate, and each experiment was repeated three times. The total length of capillary tube in wild type and gene knockout cell culture was measured in five areas with highest capillary tube density.

Flow Cytometry Analysis and Cell Sorting

Mononuclear cells from mouse blood or bone marrow were incubated with fluorescence-conjugated antibodies (fluorescein isothiocyanate (FITC) for CD34, CD117, and CD146; phycoerythrin (PE) for CD133) or isotype-matched IgG controls on ice for 30 minutes, washed with PBS, and followed by flow cytometry on a FACScan cytometer (Becton Dickinson). For cell sorting, mononuclear cells of bone marrow were stained with fluorescence-conjugated antibody (CD34-FITC and CD133-PE), and EPCs with double-positive for CD34 and CD133 were sorted by FACS StarPlus flow cytometer (Becton Dickinson). Flow cytometry data were analyzed using FCS Express software (De Novo, Los Angeles, CA).

Immunohistochemistry

Immunohistochemical staining was performed as previously described [26]. Briefly, sections (4 μm) from formalin-fixed paraffin-embedded tissues were deparaffinized in xylene. Unmasking of antigens was performed by incubating the sections in 0.01 M citrate buffer pH 6.0 in a microwave. Endogenous peroxidase was blocked by incubating sections with 3% H_2O_2. After blocking with serum and incubation with the primary antibody overnight at 4°C, sections were washed with PBS and incubated with biotinylated secondary antibody for 30 minutes at room temperature. Immunoreactivity was detected using the ABC kit (Vector, Burlingame, CA) or Envision kit (DAKO, Carpinteria, CA) for anti–mouse CD31. CD133 or CD146 staining was scored with a percentage of stromal cells with positive immunoreactivity. Microvascular density was determined by counting of CD31-positive blood vessels in three areas with the highest blood vessel density. Staining data were reviewed by two independent observers.

Pancreatic Cancer Growth in Mice

Mouse pancreatic cancer cells harboring a common Kras (G12D) mutation were mixed with Matrigel and implanted subcutaneously or orthotopically into the pancreas of 4- to 6-week-old $CXCR2^{-/-}$, $CXCR2^{+/-}$ or wild-type mice. Four weeks later, the mice were killed, harvested tumors were measured, and mouse blood and bone marrow

were collected. Tumors were fixed in 10% formalin and processed for histopathology or immunohistochemistry. Tumor volume was calculated by the following formula: tumor volume = $4/3 \times \pi A/2 \times B/2 \times C/2$, where A is the tumor's length, B is the width, and C is the height.

Statistical Analysis

Statistical comparisons were made by Student's t test or χ^2 test. $P \leq .05$ was deemed significant.

Results

Circulating EPC Level in Mouse BM and Blood

We first wanted to determine the EPC population in BM and blood of mice by FACS analysis. BM from 4-week-old CXCR2−/− mice and wild-type littermates was collected. The number of $CD34^+$ cells is slightly lower in CXCR2−/− mice than in CXCR2+/+ mice (8.5% *vs* 10%; Figure 1, *A* and *B*). However, a four-fold increase in $CD133^+$ cells and approximately two-fold increase in $CD34^+CD133^+$ cells were observed in CXCR2−/− mice compared with CXCR2+/+ mice (7.8% *vs* 1.8% and 5.2% *vs* 2.9%; Figure 1, *A* and *B*). We then determined the EPC levels in adult mice. FACS analysis was performed for CD34-, CD117-, CD133-, and CD146-positive cells on BM or blood from 12-week-old wild-type mice. We observed detectable but various levels of $CD34^+$, $CD117^+$, $CD133^+$, and $CD146^+$ EPCs, with a low level of $CD133^+$ and $CD146^+$ EPCs in the blood of wild-type adult mice (Figure 1*C*).

We examined the expression of CXCR2 in BM of wild-type and CXCR2-deficient mice (Figure 1*D*). The BM of CXCR2+/+ mouse containing 34.5% CXCR2-positive cells. The number of CXCR2-positive cells decreased to 22.5% in CXCR2+/− and was undetectable in CXCR2−/− mice.

EPC Mobilization Is Decreased in CXCR2−/− Mice in Response to Tumor Challenge

To analyze EPC mobilization in response to the pancreatic cancer challenge, we injected mouse pancreatic cancer cells into the pancreas of 4- to 6-week-old CXCR2+/+ and CXCR2−/− mice. BM or blood was collected 4 to 7 weeks after tumor transplantation for FACS analysis. In BM, the numbers of $CD34^+$, $CD117^+$, and $CD146^+$ cells were decreased in CXCR2−/− mice compared to CXCR2+/+ mice (Figure 2, *A–D*), whereas the number of $CD133^+$ cells was approximately 0.5-fold higher in CXCR2−/− mice than in CXCR2+/+ mice (2.6% *vs*

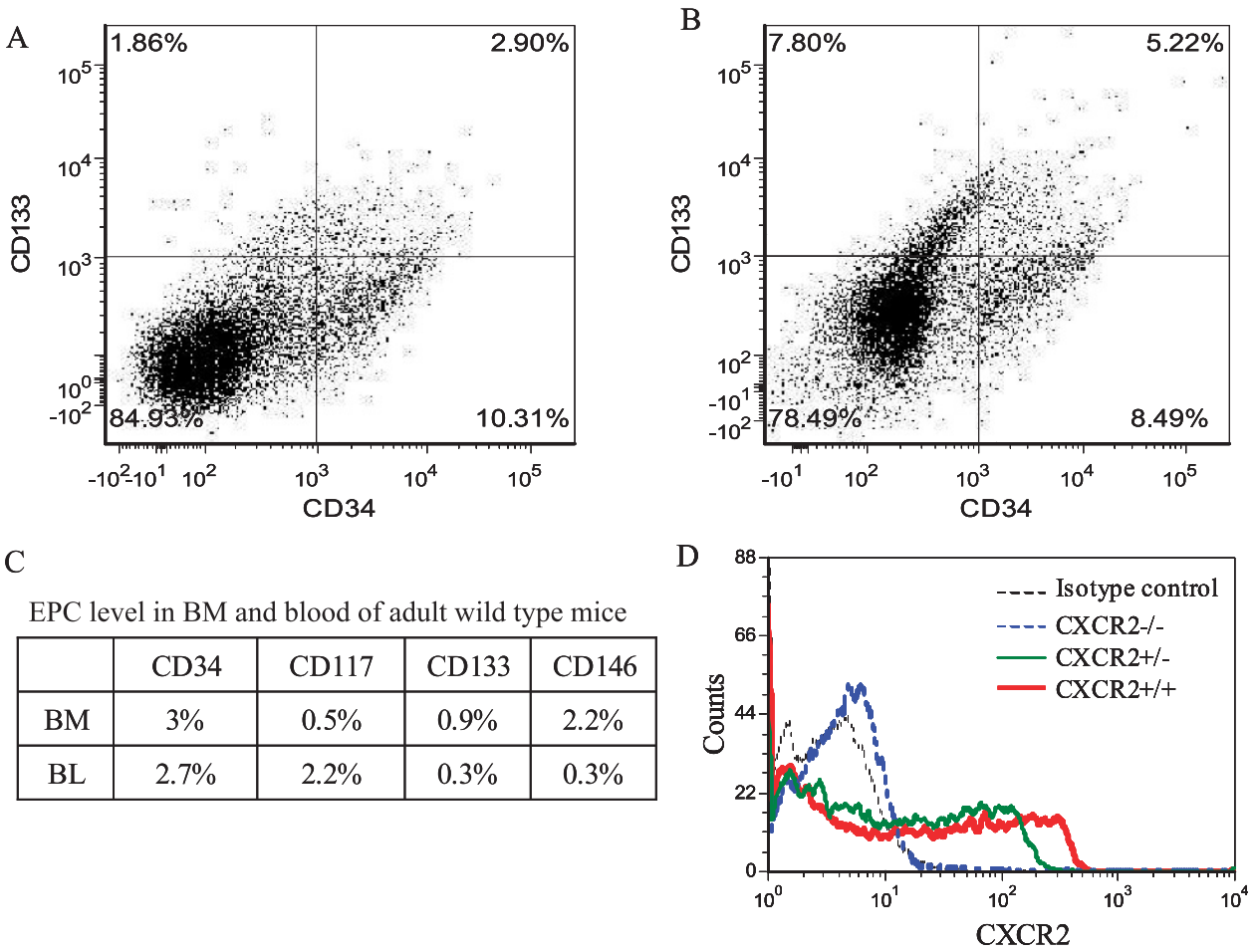

	CD34	CD117	CD133	CD146
BM	3%	0.5%	0.9%	2.2%
BL	2.7%	2.2%	0.3%	0.3%

Figure 1. Circulating levels of EPC- or CXCR2-positive cells in mice by flow cytometry analysis. EPC levels in bone marrow or blood of 4-week-old CXCR2+/+ (A) or CXCR2−/− (B) and 12-week-old wild-type mice (C). The number in the dot plot represents the percentage of positive cells (left upper, $CD133^+$; right upper, double $CD34^+$, and $CD133^+$, right low; $CD34^+$). BL indicates blood. (D) CXCR2-positive cells in CXCR2+/+ (solid, thick, and red), +/− (solid, thin, and green), and −/− (dash dot, blue) mice. Histogram represent one of the mice analyzed; n = 3–4 mice per group.

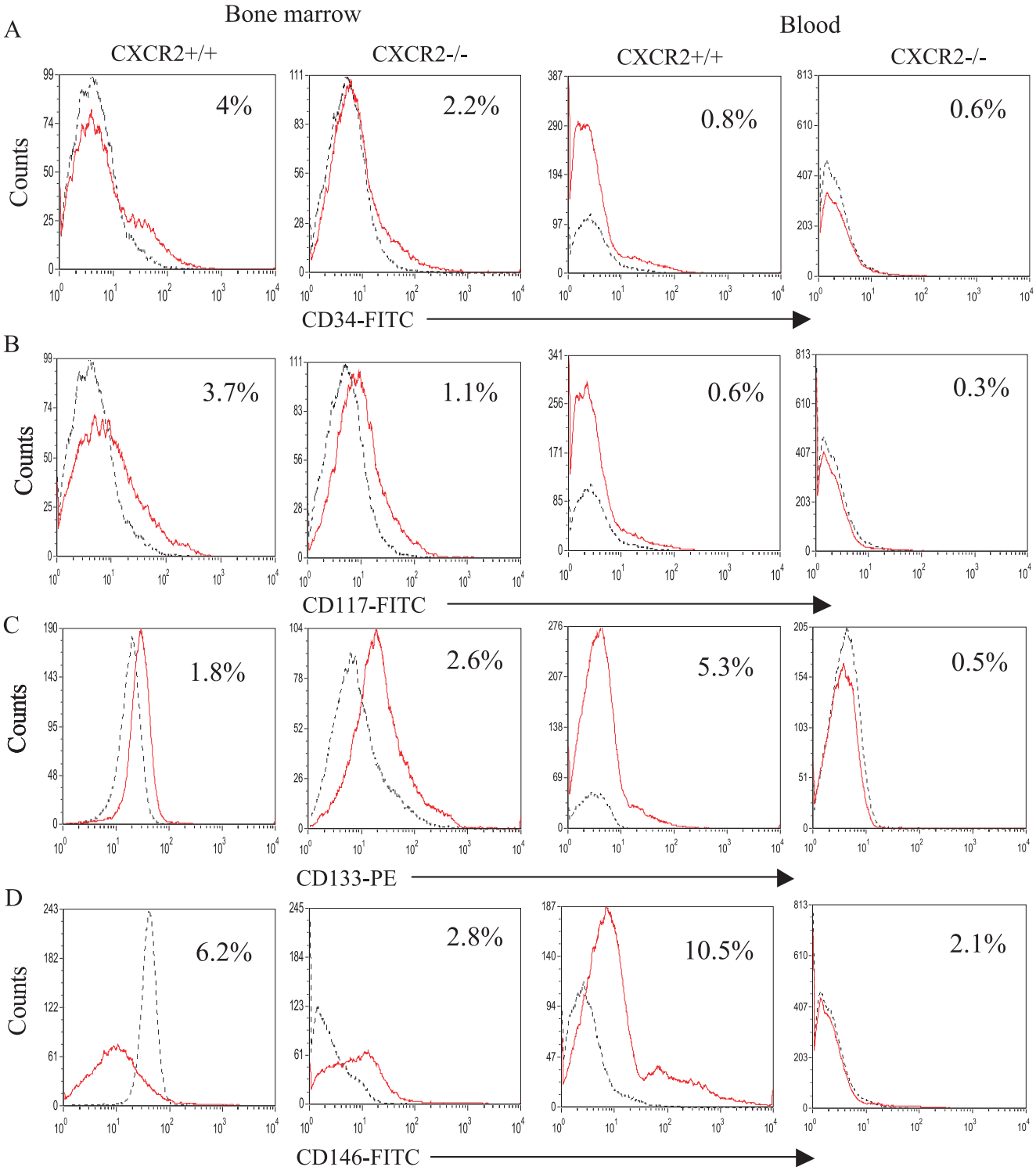

Figure 2. EPC levels in BM or blood of mice challenged with pancreatic cancer cells by flow cytometry analysis. (A) $CD34^+$ EPCs in BM or blood of CXCR2+/+ or CXCR2−/− mice. (B) $CD117^+$ EPCs in BM or blood of CXCR2+/+ or CXCR2−/− mice. (C) $CD133^+$ EPCs in BM or blood of CXCR2+/+ or CXCR2−/− mice. (D) $CD146^+$ EPCs in BM or blood of CXCR2+/+ or CXCR2−/− mice. The number on the right upper corner represents the percentage of positive cells. The red solid line is the EPC marker staining; black dashed line is the isotype control staining. Histogram represent one of the mice analyzed; n = 3–4 mice per group.

1.8%; Figure 2*C*). The rates of decrease for $CD34^+$, $CD117^+$, and $CD146^+$ cells varied from two- to three-fold in $CXCR2^{-/-}$ mice. Next, we analyzed EPC levels in the blood of CXCR2+/+ and CXCR2−/− mice. We observed slightly decreased $CD34^+$ and $CD117^+$ cells in CXCR2−/− mice. However, the level of $CD133^+$ and $CD146^+$ cells is decreased by 10- and 5-fold, respectively, in CXCR2−/− mice. These results indicate that the mobilization of $CD34^+$, $CD117^+$, $CD133^+$, and $CD146^+$ EPCs is impaired in CXCR2−/− mice.

CXCR2 Gene Knockout Reduced Proliferation, Differentiation, and Capillary-Like Structure Formation of BM-Derived Cells

To evaluate the growth rate of BM-derived EPC, BM cells were cultured with endothelial growth medium for 6 days, and cell proliferation was determined by cell count (Figure 3*A*). The cell number in CXCR2+/– cells (5.6×10^5/ml) was decreased and further reduced in CXCR2–/– (2.4×10^5/ml) compared with CXCR2+/+ cells (7.2×10^5/ml, $P < .01$ *vs* CXCR2–/– cells; Figure 3*A*). To determine the function of CXCR2 on EPC maturation and vasculogenesis, we performed an *in vitro* assay to determine the differentiation and the function of BM-derived cells. BM mononuclear cells were plated on fibronectin- (Figure 3, *B–G*) or Matrigel-coated plate (Figure 4, *A–C*) and cultured with EGM or EGM mixed with PCCM. After culturing for 4 days, CXCR2+/+ cells showed spindle cell–type differentiation in a small percentage of cells (Figure 3*B*). In contrast, no morphologically differentiation was observed in CXCR2+/– or CXCR2–/– cells on fibronectin-coated plates (Figure 3, *C* and *D*). PCCM largely increased cell differentiation of CXCR2+/+ and CXCR2+/– cells (Figure 3, *E* and *F*) but not in CXCR2–/– cells (Figure 3*G*). We observed capillary tube–like structures formed in CXCR2+/+ and CXCR2+/– cells cultured with PCCM on Matrigel at day 6 (Figure 4, *A* and *B*) but not in CXCR2–/– cell cultures (Figure 4*C*). The ability of capillary tube formation is significantly decreased in CXCR2+/– and CXCR2–/– cells (Figure 4*D*; $P < .05$ and $P < .01$). We also isolated $CD34^+$, $CD133^+$, or $CD34^+CD133^+$ cells and grew them on Matrigel-coated plates. However, no capillary tube formation was observed for up to 3 weeks with EGM or EGM plus PCCM culture, suggesting that cell-cell interactions or cellular microenvironment is important for rapid differentiation of EPCs into endothelial cells and angiogenesis.

The effect of CXCR2 deficiency on endothelial cell differentiation and angiogenesis was further examined in CXCR2 knockout mice. Pancreatic cancer cells were implanted into the pancreas of CXCR2–/–, CXCR2+/–, or CXCR2+/+ mice. CD31 staining was performed on tumor tissues. We observed a significantly decreased microvascular density in tumors grown in CXCR2–/– mice compared with CXCR2+/+ mice ($P = .03$; Figure 4, *E–G*). We also noticed that many CD31-positive cells in all the tumors analyzed do not form hollow lumens for capillary tube or veins in tumors grown in CXCR2–/– mice (Figure 4*F*) in contrast to CD31-positive cells that formed normal vessels in tumors grown in CXCR2+/+ mice (Figure 4*E*). Consistent with tumor microvascular density, the volume of the tumor in CXCR2–/– mice (0.56 cm^3) is significantly smaller than in CXCR2+/+ mice (1.5 cm^3, $P < .01$; Figure 4*H*). These data indicate a critical role of CXCR2 on EPC proliferation, differentiation, and normal vessel formation.

BM-Derived EPC Increased Pancreatic Tumor Growth In Vivo

To analyze the functional significance of BM-derived EPC in pancreatic cancer growth *in vivo*, we isolated $CD34^+CD133^+$ cells from wild-type littermate of CXCR2 mice. Mouse pancreatic cancer cells were mixed with (100:1) or without (control) EPCs and implanted into the mouse (four mice for each group) subcutaneously. We observed an increased microvascular density and tumor growth when cancer cells were mixed with EPCs (Figure 5, *A* and *B*) compared with the control. These data suggest that BM-derived EPCs promote pancreatic cancer growth.

Human Pancreatic Cancer Is Associated with Increased Expression of EPC Markers CD133 and CD146

To identify EPCs in human pancreatic cancers and normal pancreas tissues, nine cases of paired tumor-pancreas, and eight cases of unpaired tumors or normal paraffin-embedded pancreatic tissue were used for immunohistochemistry. Both CD133 and CD146 staining showed a membrane/cytoplasmic pattern (Figure 6). CD133-positive cells were observed sparsely in the normal pancreas (Figure 6*A*, *arrow*) but were increased in the stroma adjacent to cancer tissues (Figure 6*B*, *insert*; higher magnification, ×400). CD133-positive cells were limited to stromal cells. There was no obvious CD133 immunoreactivity in cancer cells. The CD146 staining was more intensive in tumor stroma (Figure 6*D*) than in normal pancreas stroma (Figure 6*C*). CD146 staining was observed in stromal cells, capillaries, and veins as well (Figure 6, *C* and *D*, *arrow*). The number of $CD133^+$ cells

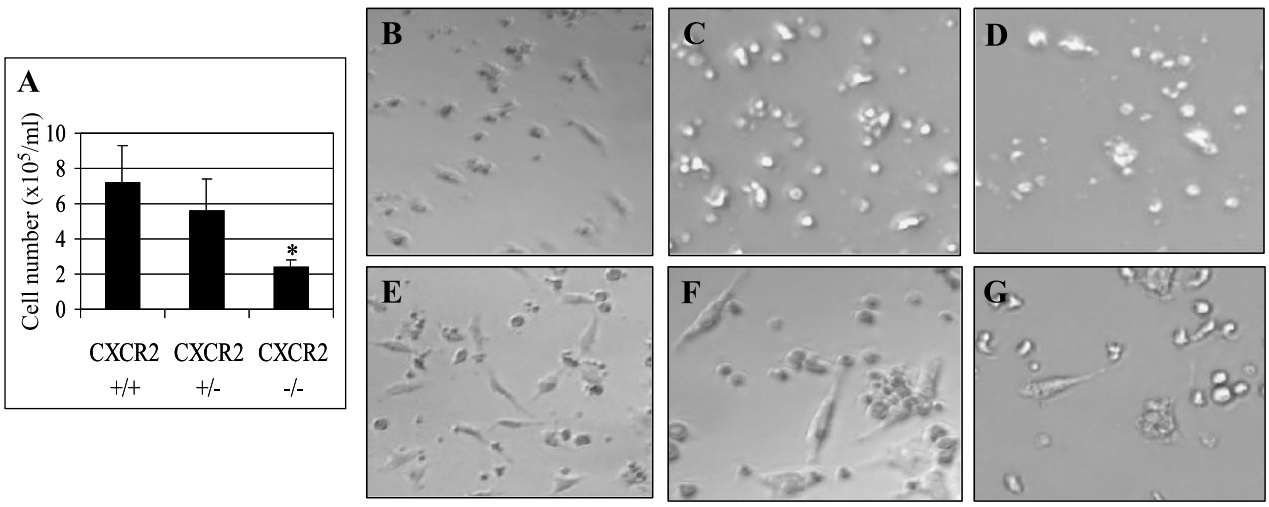

Figure 3. CXCR2 gene knockout reduced proliferation and differentiation of BM-derived EPC. (A) Cell proliferation of CXCR2 +/+, +/−, and −/− cells. Values are mean tumor volume ± SD. (B–G) Differentiation of CXCR2 +/+ (B and E), +/− (A and F), and −/− cells (D and G) grown on fibronectin-coated plate cultured with EGM (B, C, D) or EGM plus PCCM (E, F, G). *$P < 01$. Magnification, ×100.

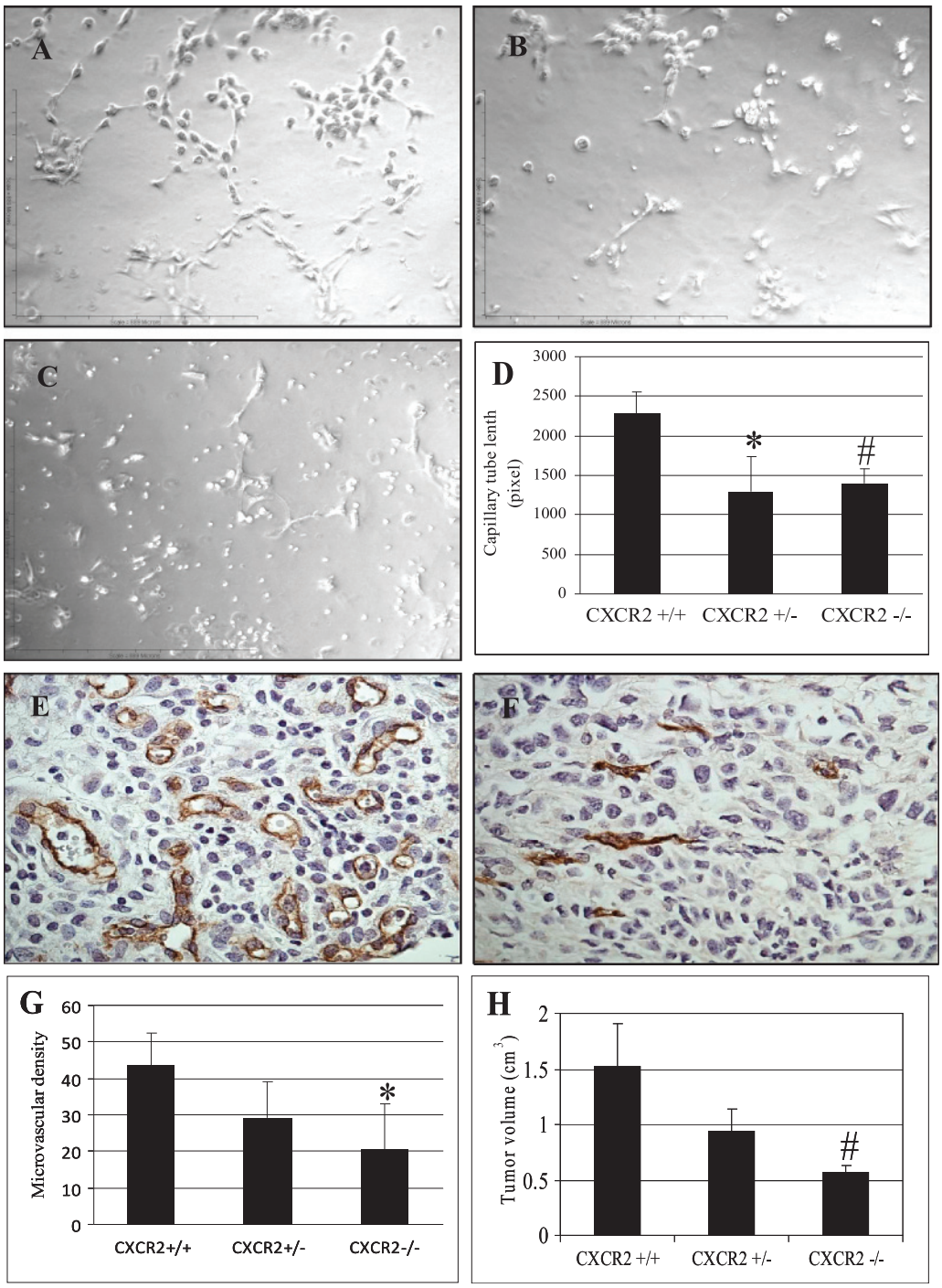

Figure 4. CXCR2 gene knockout inhibited capillary tube formation *in vitro*, decreased tumor neovascularization and tumor growth *in vivo*. (A–C) Capillary tube formation of BM-derived EPCs with CXCR2 +/+ (A), +/− (B) or −/− (C) grown on matrigel coated plate. Magnification, 100×. (D) Representative bar graph of capillary tube formation (E–G). Tumor vessel formation in CXCR2+/+ (E) and CXCR2−/− (F) mice and the representative bar graph of microvascular density (G). (H) Representative bar graph of tumor volume. n = 3–4 mice per group. Magnification, ×200. The values are mean volume ± SD. $^{*}P < .05$, $^{\#}P < .01$.

was increased in 9 (60%, $P = .002$) of 15 tumor specimens. Of 15 cancers, 11 (73.3%, $P = .0002$) showed increased CD146^{+} cells compared to normal pancreas (Table 1). In addition, all six tumors with CD133-positive cells were well to moderately differentiated, whereas nine tumors with strong CD133 staining were poorly differentiated. These data suggested that CD133 and CD146 might play a role in human pancreatic cancer growth.

Discussion

In this study, we report that the circulating CD34^{+}, CD117^{+}, CD133^{+}, and CD146^{+} EPCs are decreased in the bone marrow and/or blood of CXCR2 knockout mice in response to pancreatic cancer cell challenge. Ablation of CXCR2 gene expression slowed proliferation, differentiation, and vasculogenesis of BM-derived EPCs. BM-derived EPCs increased tumor angiogenesis and pancreatic cancer growth *in vivo*.

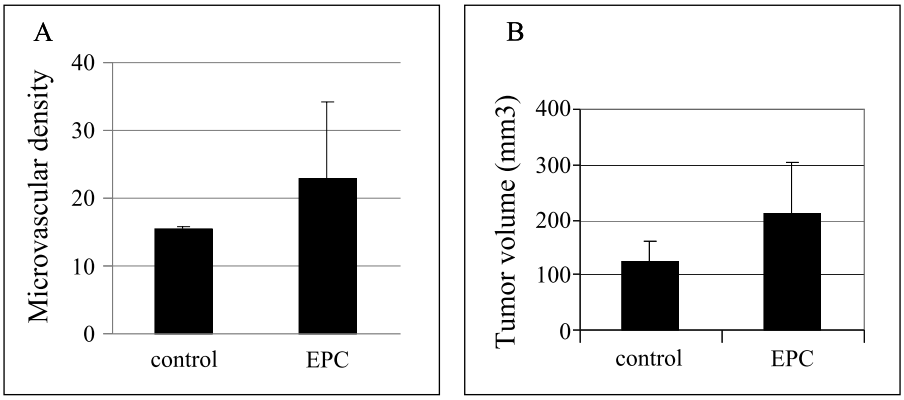

Figure 5. EPC increased microvascular density and pancreatic cancer growth *in vivo*. $CD34^+CD133^+$ cells isolated from wild-type mice were cotransplanted with mouse pancreatic cancer cells. (A) Microvascular density. (B) Tumor volume.

Human pancreatic cancer tissue revealed increased $CD133^+$ and $CD146^+$ cells compared with normal pancreas.

Recent evidence indicates an important role of BM-derived EPCs in tumor growth and metastasis. EPCs were demonstrated to incorporate into blood vessels of early stage tumor and contributed to growth and metastasis in breast cancer, melanoma, lung cancer, and insulinoma [13–16]. Ablation of EPC with anti–VE-cadherin, an antibody specifically targeting VE-cadherin decreased tumor vasculogenesis and markedly inhibited tumor growth [14]. In our study, coinjection of pancreatic cancer cells with BM-derived $CD34^+$ $CD133^+$ EPCs increased microvascular density and tumor growth, suggesting a role of BM-derived EPCs in tumor neovascularization in pancreatic adenocarcinomas.

The molecular mechanism involved in EPC-induced tumor vasculogenesis is poorly understood. Vascular endothelial growth factor (VEGF) and placental growth factor (PlGF) have been shown to contribute to EPC mobilization and homing into tumors [27]. Several reports suggested the implication of cytokines, chemokines, hypoxia-inducible 1, integrin, and matrix metalloproteinase 9 (MMP9) in regulating tumor vasculogenesis [16,17,28–32]. Recent studies indicated a role of CXC chemokine receptor ligands CXCL1, CXCL2, CXCL5, and CXCL8 in BM-derived hematopoietic progenitor cell mobilization. CXCL5/CXCR2 recruit $Gr\text{-}1^+$ $CD11b^+$ cells that have been shown to be involved in neovascularization directly or indirectly and promote tumor cell invasion and metastasis [28]. CXCL2 (Gro-β) rapidly mobilized $CD34^+$, $SCA1^+$, and $c\text{-}kit^+$ bone marrow cells [33], whereas CXCL8 and CXCL1 are involved in the homing of EPC into the ischemic myocardium [34]. Our data clearly showed that CXCR2 is required for EPC mobilization during tumor growth, as the levels of all four EPC markers, CD34, CD117, CD133, and CD146,

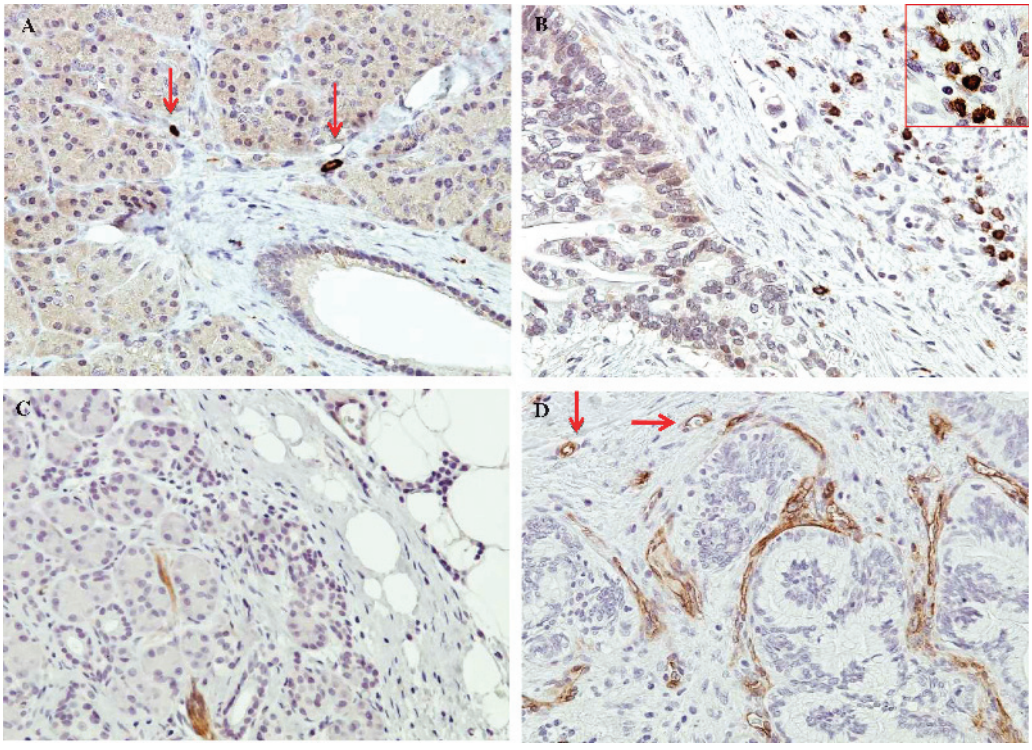

Figure 6. Immunohistochemical analysis of EPCs in human pancreatic cancer and matched normal pancreas tissue. CD133 staining in normal pancreas (A) and cancer tissue (B). CD146 staining in normal pancreas (C) and cancer tissue (D). Magnification, ×200.

Table 1. Increased CD133$^+$ and CD146$^+$ Cells in Patient Tumor Tissue.

EPC Marker	Normal	Cancer	Normal	Cancer
	CD133$^+$	CD133^{+*}	CD146$^+$	CD146$^{+\dagger}$
Paired Sample				
1	+	+	+	++
2	+	+	+	+
3	–	+	+	+++
4	–	++	–	++
5	–	++	–	–
6	+	++	+	+
7	+	++	–	–
8	+	++	–	++
9	+	+++	+	++
Unpaired Sample				
10	+		+	
11	+		–	
12		++		++/+++
13		+		++/+++
14		+		++/+++
15		++		+++
16		+		++
17		++		++

"–" indicates less than 1%; "+," between 1% and 10%; "++," greater than 10%; "+++," greater than 50% staining of tumor stroma.
*P = .02.
†P = .002.

were decreased in the circulation of tumor-bearing CXCR2–/– mice compared to wild-type mice. Although the basal level of CD133 was high in CXCR2–/– mice, the mobilization of CD133$^+$ cells was still impaired under pathologic condition, leading to a five-fold decrease in blood of CXCR2–/– compared with that of CXCR2+/+ mice (Figure 2*C*). CXCR2–/– mice have been shown to have increased number of neutrophils and B cells but not T cells, suggesting that CXCR2 may play a role in hematopoiesis, myelopoiesis, and granulocyte differentiation [35].

The impaired recruitment of hematopoietic progenitor cells including EPCs in cardiac disease and cancer indicates a critical role of CXCR2 in regulation of BM-derived progenitor cell mobilization under pathologic conditions.

The spindle cell differentiation of BM-derived cells was noticed at day 4 on fibronectin-coated culture plates. CXCR2 gene knockout slowed cell differentiation (Figure 3). PCCM increased the number of differentiated cells in CXCR2+/+ and CXCR2+/– but not in CXCR2–/– mice. The reduced angiogenic ability of EPCs under a CXCR2-deficient background was shown by a decreased capillary tube formation (Figure 3). The abnormality of tumor vessel formation in CXCR2–/– mice further indicates a role of CXCR2 in BM-derived cell differentiation into endothelial cells and angiogenesis. The contribution of BM-derived EPC to tumor growth has been demonstrated in several cancer models [12–15]. By an alternative approach, we conducted cotransplantation of EPC with pancreatic cancer cells and observed increased microvascular density and accelerated tumor growth, suggesting a role of EPC in cancer growth in our pancreatic cancer model.

Clinical evidence demonstrated that EPC level is increased in breast cancer [36], non–small cell lung cancer [37], lymphoma [38], head and neck cancer [39], myeloma [40], and hepatocellular carcinoma [41]. Furthermore, the EPC level is correlated with the clinical stage in breast cancer [36] and patient survival in lung cancer [37]. The increased number of CD133$^+$ and CD146$^+$ EPCs in patient pancreatic cancer tissues compared to normal pancreas tissue indicates that EPC might be involved in tumor neovascularization in human pancreatic cancer.

In summary, we have demonstrated that the BM-derived EPC is implicated in pancreatic cancer growth. CXCR2 is required for mobilization, proliferation, and differentiation of BM-derived CD34$^+$, CD117$^+$, CD133$^+$, or CD146$^+$ EPCs. BM-derived EPCs play a role in tumor neovascularization in pancreatic cancer. Our study also provides a cellular mechanism for CXCR2 mediated tumor angiogenesis. Furthermore, EPC may serve as a biomarker for tumor neovascularization and pancreatic cancer progression. Targeted ablation of BM-derived EPC may offer novel therapeutic strategy for tumor neovascularization and cancer progression.

References

[1] Shantsila E, Watson T, Tse HF, and Lip GY (2007). Endothelial colony forming units: are they a reliable marker of endothelial progenitor cell numbers? *Ann Med* **39**, 474–479.

[2] Lamagna C and Bergers G (2006). The bone marrow constitutes a reservoir of pericyte progenitors. *J Leukoc Biol* **80**, 677–681.

[3] Shojaei F, Wu X, Malik AK, Zhong C, Baldwin ME, Schanz S, Fuh G, Gerber HP, and Ferrara N (2007). Tumor refractoriness to anti-VEGF treatment is mediated by CD11b$^+$Gr1$^+$ myeloid cells. *Nat Biotechnol* **25**, 911–920.

[4] Conejo-Garcia JR, Benencia F, Courreges MC, Kang E, Mohamed-Hadley A, Buckanovich RJ, Holtz DO, Jenkins A, Na H, Zhang L, et al. (2004). Tumor-infiltrating dendritic cell precursors recruited by a β-defensin contribute to vasculogenesis under the influence of VEGF-A. *Nat Med* **10**, 950–958.

[5] Au P, Tam J, Fukumura D, and Jain RK (2008). Bone marrow–derived mesenchymal stem cells facilitate engineering of long-lasting functional vasculature. *Blood* **111**, 4551–4558.

[6] Condeelis J and Pollard JW (2006). Macrophages: obligate partners for tumor cell migration, invasion, and metastasis. *Cell* **124**, 263–266.

[7] Asahara T, Murohara T, Sullivan A, Silver M, van der Zee R, Li T, Witzenbichler B, Schatteman G, and Isner JM (1997). Isolation of putative progenitor endothelial cells for angiogenesis. *Science* **275**, 964–967.

[8] Wu X, Lensch MW, Wylie-Sears J, Daley GQ, and Bischoff J (2007). Hemogenic endothelial progenitor cells isolated from human umbilical cord blood. *Stem Cells* **25**, 2770–2776.

[9] Asahara T, Masuda H, Takahashi T, Kalka C, Pastore C, Silver M, Kearne M, Magner M, and Isner JM (1999). Bone marrow origin of endothelial progenitor cells responsible for postnatal vasculogenesis in physiological and pathological neovascularization. *Circ Res* **85**, 221–228.

[10] Bertolini F, Shaked Y, Mancuso P, and Kerbel RS (2006). The multifaceted circulating endothelial cell in cancer: towards marker and target identification. *Nat Rev Cancer* **6**, 835–845.

[11] Ergun S, Hohn HP, Kilic N, Singer BB, and Tilki D (2008). Endothelial and hematopoietic progenitor cells (EPCs and HPCs): hand in hand fate determining partners for cancer cells. *Stem Cell Rev* **4**, 169–177.

[12] Lyden D, Hattori K, Dias S, Costa C, Blaikie P, Butros L, Chadburn A, Heissig B, Marks W, Witte L, et al. (2001). Impaired recruitment of bone-marrow–derived endothelial and hematopoietic precursor cells blocks tumor angiogenesis and growth. *Nat Med* **7**, 1194–1201.

[13] Kaplan RN, Riba RD, Zacharoulis S, Bramley AH, Vincent L, Costa C, MacDonald DD, Jin DK, Shido K, Kerns SA, et al. (2005). VEGFR1-positive haematopoietic bone marrow progenitors initiate the pre-metastatic niche. *Nature* **438**, 820–827.

[14] Nolan DJ, Ciarrocchi A, Mellick AS, Jaggi JS, Bambino K, Gupta S, Heikamp E, McDevitt MR, Scheinberg DA, Benezra R, et al. (2007). Bone marrow–derived endothelial progenitor cells are a major determinant of nascent tumor neovascularization. *Genes Dev* **21**, 1546–1558.

[15] Gao D, Nolan DJ, Mellick AS, Bambino K, McDonnell K, and Mittal V (2008). Endothelial progenitor cells control the angiogenic switch in mouse lung metastasis. *Science* **319**, 195–198.

[16] Spring H, Schuler T, Arnold B, Hammerling GJ, and Ganss R (2005). Chemokines direct endothelial progenitors into tumor neovessels. *Proc Natl Acad Sci USA* **102**, 18111–18116.

[17] Du R, Lu KV, Petritsch C, Liu P, Ganss R, Passegue E, Song H, Vandenberg S, Johnson RS, Werb Z, et al. (2008). HIF1α induces the recruitment of bone

marrow–derived vascular modulatory cells to regulate tumor angiogenesis and invasion. *Cancer Cell* **13**, 206–220.

[18] Raman D, Baugher PJ, Thu YM, and Richmond A (2007). Role of chemokines in tumor growth. *Cancer Lett* **256**, 137–165.

[19] Singh S, Sadanandam A, and Singh RK (2007). Chemokines in tumor angiogenesis and metastasis. *Cancer Metastasis Rev* **26**, 453–467.

[20] Miyazaki H, Patel V, Wang H, Edmunds RK, Gutkind JS, and Yeudall WA (2006). Down-regulation of CXCL5 inhibits squamous carcinogenesis. *Cancer Res* **66**, 4279–4284.

[21] Manna SK and Ramesh GT (2005). Interleukin-8 induces nuclear transcription factor-κB through a TRAF6-dependent pathway. *J Biol Chem* **280**, 7010–7021.

[22] Begley LA, Kasina S, Mehra R, Adsule S, Admon AJ, Lonigro RJ, Chinnaiyan AM, and Macoska JA (2008). CXCL5 promotes prostate cancer progression. *Neoplasia* **10**, 244–254.

[23] Li A, Dubey S, Varney ML, Dave BJ, and Singh RK (2003). IL-8 directly enhanced endothelial cell survival, proliferation, and matrix metalloproteinases production and regulated angiogenesis. *J Immunol* **170**, 3369–3376.

[24] Li A, Varney ML, and Singh RK (2001). Expression of interleukin 8 and its receptors in human colon carcinoma cells with different metastatic potentials. *Clin Cancer Res* **7**, 3298–3304.

[25] Funahashi H, Satake M, Dawson D, Huynh NA, Reber HA, Hines OJ, and Eibl G (2007). Delayed progression of pancreatic intraepithelial neoplasia in a conditional Kras(G12D) mouse model by a selective cyclooxygenase-2 inhibitor. *Cancer Res* **67**, 7068–7071.

[26] Li A, Hasui K, Yonezawa S, Tanaka S, and Sato E (1999). Immunohistochemical analysis of pericryptal fibroblast sheath and proliferating epithelial cells in human colorectal adenomas and carcinomas with adenoma components. *Pathol Int* **49**, 426–434.

[27] Li B, Sharpe EE, Maupin AB, Teleron AA, Pyle AL, Carmeliet P, and Young PP (2006). VEGF and PlGF promote adult vasculogenesis by enhancing EPC recruitment and vessel formation at the site of tumor neovascularization. *FASEB J* **20**, 1495–1497.

[28] Yang L, Huang J, Ren X, Gorska AE, Chytil A, Aakre M, Carbone DP, Matrisian LM, Richmond A, Lin PC, et al. (2008). Abrogation of TGFβ signaling in mammary carcinomas recruits Gr-1^{+}CD11b^{+} myeloid cells that promote metastasis. *Cancer Cell* **13**, 23–35.

[29] Jin DK, Shido K, Kopp HG, Petit I, Shmelkov SV, Young LM, Hooper AT, Amano H, Avecilla ST, Heissig B, et al. (2006). Cytokine-mediated deployment of SDF-1 induces revascularization through recruitment of CXCR4^{+} hemangiocytes. *Nat Med* **12**, 557–567.

[30] Shojaei F, Wu X, Zhong C, Yu L, Liang XH, Yao J, Blanchard D, Bais C, Peale FV, van Bruggen N, et al. (2007). Bv8 regulates myeloid-cell–dependent tumour angiogenesis. *Nature* **450**, 825–831.

[31] Du R, Petritsch C, Lu K, Liu P, Haller A, Ganss R, Song H, Vandenberg S, and Bergers G (2008). Matrix metalloproteinase-2 regulates vascular patterning and growth affecting tumor cell survival and invasion in GBM. *Neuro Oncol* **10**, 254–264.

[32] Ahn GO and Brown JM (2008). Matrix metalloproteinase-9 is required for tumor vasculogenesis but not for angiogenesis: role of bone marrow–derived myelomonocytic cells. *Cancer Cell* **13**, 193–205.

[33] Pelus LM and Fukuda S (2006). Peripheral blood stem cell mobilization: the CXCR2 ligand GROβ rapidly mobilizes hematopoietic stem cells with enhanced engraftment properties. *Exp Hematol* **34**, 1010–1020.

[34] Hristov M, Zernecke A, Bidzhekov K, Liehn EA, Shagdarsuren E, Ludwig A, and Weber C (2007). Importance of CXC chemokine receptor 2 in the homing of human peripheral blood endothelial progenitor cells to sites of arterial injury. *Circ Res* **100**, 590–597.

[35] Cacalano G, Lee J, Kikly K, Ryan AM, Pitts-Meek S, Hultgren B, Wood WI, and Moore MW (1994). Neutrophil and B cell expansion in mice that lack the murine IL-8 receptor homolog. *Science* **265**, 682–684.

[36] Naik RP, Jin D, Chuang E, Gold EG, Tousimis EA, Moore AL, Christos PJ, de Dalmas T, Donovan D, Rafii S, et al. (2008). Circulating endothelial progenitor cells correlate to stage in patients with invasive breast cancer. *Breast Cancer Res Treat* **107**, 133–138.

[37] Dome B, Timar J, Dobos J, Meszaros L, Raso E, Paku S, Kenessey I, Ostoros G, Magyar M, Ladanyi A, et al. (2006). Identification and clinical significance of circulating endothelial progenitor cells in human non–small cell lung cancer. *Cancer Res* **66**, 7341–7347.

[38] Igreja C, Courinha M, Cachaco AS, Pereira T, Cabecadas J, da Silva MG, and Dias S (2007). Characterization and clinical relevance of circulating and biopsy-derived endothelial progenitor cells in lymphoma patients. *Haematologica* **92**, 469–477.

[39] Brunner M, Thurnher D, Heiduschka G, Grasl M, Brostjan C, and Erovic BM (2008). Elevated levels of circulating endothelial progenitor cells in head and neck cancer patients. *J Surg Oncol* **98**, 545–550.

[40] Zhang H, Vakil V, Braunstein M, Smith EL, Maroney J, Chen L, Dai K, Berenson JR, Hussain MM, Klueppelberg U, et al. (2005). Circulating endothelial progenitor cells in multiple myeloma: implications and significance. *Blood* **105**, 3286–3294.

[41] Yu D, Sun X, Qiu Y, Zhou J, Wu Y, Zhuang L, Chen J, and Ding Y (2007). Identification and clinical significance of mobilized endothelial progenitor cells in tumor vasculogenesis of hepatocellular carcinoma. *Clin Cancer Res* **13**, 3814–3824.